Dynamic Analysis of the Two-Bladed Horizontal Axis Wind Turbine

Shigemitsu AOKI[+1], Tetsuya KOGAKI[+2] and Kenichi SAKURAI [+3]

[+1] AIST Invited Research Scientist, National Institute of Advanced Industrial Science and Technology (AIST) Renewable Energy Research Center (RENRC), 2-2-9 Machiikedai, Koriyama, Fukushima, 963-0298, Japan
[+2] Team Leader, National Institute of Advanced Industrial Science and Technology (AIST)
[+3] Technical Staff, National Institute of Advanced Industrial Science and Technology (AIST)

ABSTRACTS

In order to make an approach according to the dynamic characteristics of the two-bladed Horizontal axis wind turbine, that is substantially unstable and non-linear motion, the basic equations were derived by Lagrange's method on Eulerian coordinate system.

An aero-elastic simulation model named AIST-RAM (AIST Real-Time Model), that represents characteristics of the motion was developed referring to the basic equations and another factors such as an aerodynamic force acting on the blades that is strongly affected by the motion and elasticity of the blades itself.

Also, a scale model of the multi-megawatt horizontal-axis wind turbine was constructed as well as the specified management system called Hard-wear in the Loop (HIL).

Through the successive evaluation by wind-tunnel testing and field testing accompanied with real-time simulation arranged by the Hard-wear in the Loop System, the credibility of the simulation soft-wear is gradually confirmed along with the clear understanding as to a characteristics of the teetered-hub system that has ever been discussed among the industry.

Keyword: Two-Bladed Horizontal Axis Wind Turbine, Basic Equations, Lagrange's Method, Eulerian coordinate system, Real-time Simulation, Hard-wear in the Loop System.

1. Introduction

Multi-megawatt scale Horizontal-Axis Wind Turbine is getting larger and larger revealing the conceptual design of over 200 meter diameter scale recently.

Whereas, the consideration to apply two-bladed rotor instead of current there-bladed design is under discussion, pros. and cons. of the design is recognized as

Pros.

  a) Possibly reduce the weight of the system.

  b) Design constraint for the increasing gear is relaxed with higher rotational speed.

  c) The aerodynamic load in extreme wind condition could be reduced.

Cons.

  d) There are significant difference of the inertial force and/or aerodynamic force according to the blade-position.

  e) Power coefficient of the rotor is inferior.

Recently, although the studies and researches [1][2] according to the teetered hub is upcoming, there are few which applied current advanced technology of evaluation for the system.

In this study, through the successive evaluation by wind-tunnel testing and field testing accompanied with real-time simulation system arranged by the Hard-wear in the Loop System, the credibility of the simulation

[+1]s.aoki@aist.go.jp, [+2]kogaki.t@aist.go.jp, [+3]kenichi-sakurai@aist.go.jp

soft-wear is gradually confirmed along with the clear understanding as to a characteristics of the teetered-hub system

2. Lagrange's Method

2.1 Coordinate system

In order to introduce the basic equations that ordinate the inertial force acting on the system, "Eulerian coordinate system[3]" was adopted as a generalized coordinates. Basic attitude of the rotor-blade was conducted with four degree of freedom defined as β, ψ, θ and ϕ, as is shown in Figure 1.

Hence β is defined as the pitch angle that adjust the attack angle around the axis approximately put on the aerodynamic center of each blade section, ψ is defined as the azimuth angle of the blade rotating on the main axis of the rotor, θ is defined as the tilt angle that starts from perpendicular position and ϕ is defined as yaw angle of the main axis according to the directional change.

Furthermore in this study, τ is defined as teeter-angle that allows pendulum like motion between the pitch axis of the blades and the main axis, accompany with delta-three (δ_3) angle for the adjustment between the pitch axis and the teeter axis.

Also in Figure 1, u is the wind speed, a is the distance between the hub-center and the base point of the coordinate system, b is the distance between the gravity-center of the blade and the hub-center, m_1 is mass of the blade, I is moment of inertia around the rotor axis, J is moment of inertia around the pitch axis respectively.

In addition, a small amount of mass m_2 is assumed with the distance c from the hub-center, in order to make the adjustment of mass-balance of the rotor according to the teeter-axis.

$$\omega_2 = \dot{\beta} - \dot{\theta}\sin\psi + \dot{\phi}\cos\psi\sin\theta$$
$$\omega_1 = \dot{\psi} + \dot{\phi}\cos\theta$$

δ_3: delta-three angle

ϕ: yaw angle

τ: teeter angle

ψ: azimuth θ: tilt angle
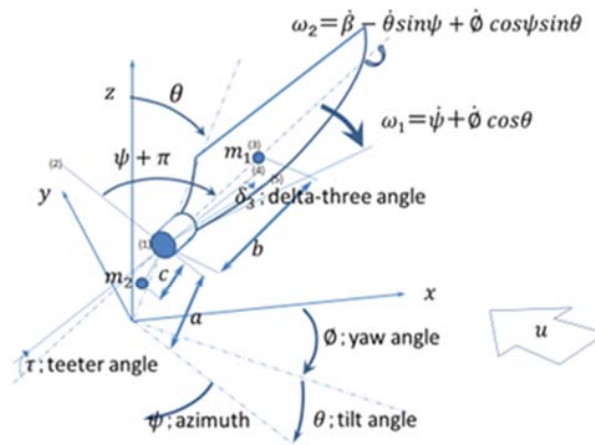
Figure 1: Fundamental coordinate system (Euler)

2.2 Potential energy of the system

Considering the effect of the gravitational acceleration, potential energy related to m_1 is written as equation (1), as to m_2, equation (2), and as a result, summary of the potential energy according to Lagrange's function is written as equation (3).

$$V_1 = m_1 g[a\,\cos\theta - b\cos(\psi + \delta_3)\sin\theta - b\,\sin\tau\cos\theta + b(1 - \cos\tau)\sin\theta\cos(\psi + \delta_3)] \qquad (1)$$

$$V_2 = m_2 g[(a - c \cos \tau) \cos \theta + c \sin \tau \cos \psi \sin \theta] \tag{2}$$

$$V = V_1 + V_2 \tag{3}$$

2.3 Kinetic energy of the system

2.3.1 According to yaw axis (ϕ system)

2.3.1.1 as to m_1

Contribution to $\dot{\phi}$, $a \sin \theta \, \dot{\phi}$,

Similarly, contribution of $\dot{\psi}$ is through $\frac{\partial \psi}{\partial t} [b \sin(\psi + \delta_3)]$ $b \cos(\psi + \delta_3) \dot{\psi}$,

Also, contribution of $\dot{\tau}$ is through $\frac{\partial \tau}{\partial t} [b \sin \tau \sin \theta \sin(\psi + \delta_3)]$ $b \cos \tau \sin \theta \sin(\psi + \delta_3) \dot{\tau}$,

Considering the components above, following equation is derived.

$$E_1 = \frac{1}{2} m_1 \big[a \sin \theta \, \dot{\phi} + b \cos(\psi + \delta_3) \dot{\psi} + \ \ b \cos \tau \sin \theta \sin(\psi + \delta_3) \dot{\tau} \big]^2 \tag{4}$$

2.3.1.2 as to m_2

Contribution to $\dot{\phi}$, $[a \sin \theta - c \cos \tau \, \sin \theta - c \, \sin \tau \cos \theta + c \, \sin \tau \, \cos(\psi + \delta_3) \cos \theta] \dot{\phi}$,

Similarly, of $\dot{\psi}$ is through $\frac{\partial \psi}{\partial t} [c \, \sin \tau \cos(\psi + \delta_3)]$, $-c \sin \tau \sin(\psi + \delta_3) \dot{\psi}$

Derived equation is written as

$$E_2 = \frac{1}{2} m_2 \big\{ [a \sin \theta - c \cos \tau \sin \theta - c \sin \tau \cos \theta + c \sin \tau \cos(\psi + \delta_3) \cos \theta] \, \dot{\phi} - c \sin \tau \sin(\psi + \delta_3) \, \dot{\psi} \big\}^2$$
$$\tag{5}$$

2.3.1.3 as to I

Projected length of the blade length (R) around yaw axis on the $\emptyset$-plane is, $(R) sin(\psi + \delta_3)$

Contribution of $\dot{\psi}$ is $\cos(\psi + \delta_3) \, \dot{\psi}$

Derived equation is written as

$$E_3 = \frac{1}{2} I [sin \, (\psi + \delta_3) \dot{\emptyset} + cos(\psi + \delta_3) \dot{\psi}] \tag{6}$$

2.3.1.4 as to J

This component seems to be not effective considering that $J/I \ll 1$.

2.3.2 According to tilt axis (θ system)

2.3.2.1 as to m_1

Contribution to $\dot{\theta}$, $a \dot{\theta}$,

As to the contribution of $\dot{\psi}$ is, considering the tangential component as $b \, \cos(\psi + \delta_3)$,

Through the calculation $\frac{\partial \psi}{\partial t} [b \cos(\psi + \delta_3)]$ $-b \sin(\psi + \delta_3) \, \dot{\psi}$,

Derived equation is written as

$$E_4 = \frac{1}{2} m_1 \big[a \dot{\theta} - b \, \sin(\psi + \delta_3) \, \dot{\psi} \big]^2 \tag{7}$$

2.3.2.2 as to m_2

Contribution to $\dot{\theta}$, $a\dot{\theta}$,

Contribution of $\dot{\psi}$ is through $\frac{\partial \psi}{\partial_t}[-c \sin \tau \cos(\psi + \delta_3)]$ $c \sin \tau \sin(\psi + \delta_3)\,\dot{\psi}$,

Derived equation is written as

$$E_5 = \frac{1}{2}m_2\big[a\dot{\theta} + c \sin \tau \sin (\psi + \delta_3)\dot{\psi}\big]^2 \tag{8}$$

2.3.2.3 as to I

Projected length of the blade length (R) around tilt axis on the θ-plane is, $(R) \cos(\psi + \delta_3)$,

Contribution of $\dot{\psi}$ is $-sin(\psi + \delta_3)\dot{\psi}$

Derived equation is written as

$$E_6 = \frac{1}{2}I\big[\cos (\psi + \delta_3)\dot{\theta} - \sin(\psi + \delta_3)\dot{\psi}\big]^2 \tag{9}$$

2.3.2.4 as to J

This component seems also to be not effective considering that $J/I \ll 1$.

2.3.3 According to azimuth (ψ system)

2.3.3.1 as to m_1

Following the definition according to the Eulerian coordinate system, derived equation is

$$E_7 = \frac{1}{2}m_1 b^2 \cos^2 \tau \left(\dot{\psi} + \cos\theta \, \dot{\varnothing}\right)^2 \tag{10}$$

2.3.3.2 as to m_2

Similarly, $E_8 = \frac{1}{2}m_2 c^2 \sin^2 \tau \left(\dot{\psi} + \cos\theta \, \dot{\varnothing}\right)$ (11)

2.3.3.3 as to I

Also, $E_9 = \frac{1}{2}I \cos^2 \tau \left(\dot{\psi} + \cos\theta \, \dot{\varnothing}\right)^2$ (12)

2.3.4 According to pitch axis (β system)

2.3.4.1 as to J

Following the definition according to the Eulerian coordinate system in case that the effect of teetering is negligible, derived equation is,

$$E_{10} = \frac{1}{2}J\big(\dot{\beta} - \sin\psi\dot{\theta} + \cos \psi \, \sin\theta\dot{\Phi}\big)^2 \tag{13}$$

2.4 Lagrange's function

Summary, the Lagrange's function of the system is calculated by following equation, with the notation of n ; 1〜9, m ; 2.

$$\boldsymbol{L = T - V = \sum E_n - \sum V_m} \tag{14}$$

Assuming that each degree of freedom as independent variable q, series of basic equations are derived by following formula.

$$\frac{d}{dt}\left(\frac{\partial L}{\partial \dot{q}}\right) - \frac{\partial L}{\partial q} = O \tag{15}$$

3. Basic equations

3.1 Basic equations

Set of differential equation are derived,

As to yaw（ϕ）system,

$$k_{11}\ddot{\phi} + k_{12}\dot{\phi}\dot{\psi} + k_{17}\ddot{\psi} + k_{18}\dot{\psi}^2 + k_{19}\dot{\psi}\dot{\tau} + k_{1a}\ddot{\tau} = 0 \tag{16}$$

As to tilt（θ）system,

$$k_{22}\dot{\phi}\dot{\psi} + k_{24}\dot{\phi}\dot{\theta} + k_{25}\ddot{\theta} + k_{26}\dot{\theta}\dot{\psi} + k_{27}\ddot{\psi} + k_{28}\dot{\psi}^2 + k_{29}\dot{\psi}\dot{\tau} + k_{2a}\ddot{\tau} + k_{2b}g = 0 \tag{17}$$

As to azimuth（ψ）system,

$$k_{31}\ddot{\phi} + k_{32}\dot{\phi}\dot{\psi} + k_{33}\dot{\phi}\dot{\tau} + k_{37}\ddot{\psi} + k_{39}\dot{\psi}\dot{\tau} + k_{3b}g = 0 \tag{18}$$

As to teeter（τ）system,

$$k_{41}\ddot{\phi} + k_{42}\dot{\phi}\dot{\psi} + k_{48}\dot{\psi}^2 + k_{4a}\ddot{\tau} + k_{4b}g = 0 \tag{19}$$

3.2 Coefficients.

Coefficients for each term can be arranged like in Table 1.

Table 1: Coefficients of each term.

	ϕ system	θ system	ψ system	τ system		ϕ system	θ system	ψ system	τ system
$\ddot{\phi}$	k_{11}		k_{31}	k_{41}	$\dot{\theta}\dot{\psi}$		k_{26}		
$\dot{\phi}\dot{\psi}$	k_{12}	k_{22}	k_{32}	k_{42}	$\ddot{\psi}$	k_{17}	k_{27}	k_{37}	
$\dot{\phi}\dot{\tau}$			k_{33}		$\dot{\psi}^2$	k_{18}	k_{28}		k_{48}
$\dot{\phi}\dot{\theta}$		k_{24}			$\dot{\psi}\dot{\tau}$	k_{19}	k_{29}	k_{39}	
$\ddot{\theta}$		k_{25}			$\ddot{\tau}$	k_{1a}	k_{2a}		k_{4a}
$\dot{\theta}\dot{\psi}$		k_{26}			g		k_{2b}	k_{3b}	k_{4b}

Hence, coefficient k_{11}, k_{25}, k_{37}, k_{4a} are principal moment of inertia for $\phi\square$system, θ system,$\square\psi$ system and τ system

k_{*8}・・are related to the centrifugal force that causes significant acceleration in general.

k_{*2}・・, k_{*3}・・, k_{*4}・・, k_{*6}・・, k_{*9}・・are related to components oriented by coupled angular velocities, and in case, for example, related to k_{22}, k_{33}, k_{29}, the angular acceleration consists of angular velocities of normal axes, it causes gyro-moment.

Coriolis' force is caused in the other cases.

k_{*b} are related to gravitational acceleration.

In this study, influence of the pitch movement for the inertial property was neglected, respectively.

4. Simulation model construction

4.1 Modeling circumstances

A circumstances of time-driven simulation system was prepared to establish the construction of the model shown in Figure 2.
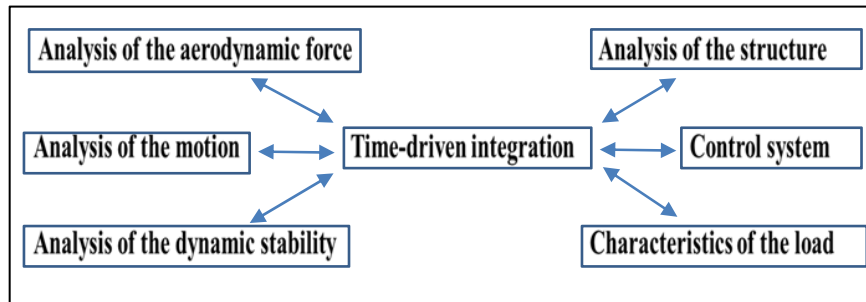
Figure 2 : Structure of the Model

4.2 Inner force implementation

At first, inertial forces derived by consequential basic equations shown as formula (16), (17), (18) and (19) are implemented as inner force of the system.

4.3 Outer force implementation

4.3.1 Effect of the elasticity of the Tower and the Blade(s)

As to the deflection of the tower, following equation of first order bending was applied.

$$\tfrac{1}{2}\rho(u-\dot{x})^2 A C_T - \tfrac{3EI}{l^3}x = \left(m_N + \tfrac{3EI}{l^3}\tfrac{1}{w^2}\right)\ddot{x} \tag{20}$$

Hence, x is the deflection of the tower at the tower-top, namely the displacement of the main-shaft, ρ is the density of the air, A is the swept area of the rotor, C_T is the thrust coefficient of the rotor, EI is the rigidity of the tower for bending, l is the length of tower, m_N is the mass of tower-top, and w is the mass of tower per unit length.

Similarly, as to the effect of blade-deflection, applying the characteristics of the blade of which used as a scale model for the experiment, result of following equation was used to compensate the teeter motion.

$$2m_1\left[0.0035\ddot{W} + \ddot{x} + 0.53l\ddot{t}\right] = \tfrac{1}{2}\rho\left[u - 0.048\dot{W}\right]^2 A C_t \tag{21}$$

Hence, W is deflection of the blade-tip, respectively.

4.3.2 Effect of the aerodynamic-force of the rotor-blade(s)

In order to apply the aerodynamic-force of the rotor-blade, aerodynamic torque-coefficient by following equation referring to the characteristics of standard blade design was adopted.

$$C_q = 0.079 + \tfrac{0.08}{(\beta+2)} - [5.5 + 0.007(\beta + 2)^{2.5}]\lambda \times 10^{-3} \tag{22}$$

4.3.3 Compensation of the effect of aerodynamic-force

Representative factors as follows were considered to be significant and implemented to adjust the torque-coefficient accompany with the variation of λ(tip-speed ratio) and β.

・Δu (variation of hub wind-speed)　　；coherent variation of wind-speed around the rotor-disc

・$\dot{x}$ (deflection-speed of tower-head)　；deflection speed of tower-head parallel to the wind speed

$\cdot u_{local}$ (wind-speed distribution)   ; effect of the wind speed distribution like wind shear

$\cdot r\dot{t}$ (teetering motion)   ; relative variation of wind speed due to the teeter motion

$\cdot r\dot{\emptyset}$ (yaw movement)   ; relative variation of wind speed due to the yaw motion

4.3.4 Effects of another outer force

  Effects of actuators like driving-motor of main shaft, that of yawing and that of pitch-axis are implemented to ψ system, ϕ system and β system, based on the D'Alembert's principle as well as the various kind of aerodynamic force as is shown in current Simulation Model[4].

5．Test facilities for evaluation

5.1 Over view

  Figure 3 shows a scale-model of the wind-turbine and a controller, a power source for driving, measurement system with HILS system and Host computer.

Figure 3   Experimental system for Evaluation

  Figure 4 shows basic specifications of the wind-tunnel and the model for this study.

Figure 4 Basic specifications of the wind tunnel testing

5.2 HILS system

   HILS system was invented as a tool for model-base design technology.

   As is shown in Figure 5, the main facility of such a system is to exchange the data between one which was measured at hard-wear and the corresponding result of the real-time simulation in order to make a precise and quick comparison.

   In order to realize it, the simulation soft-wear is required an ability of real-time simulation.
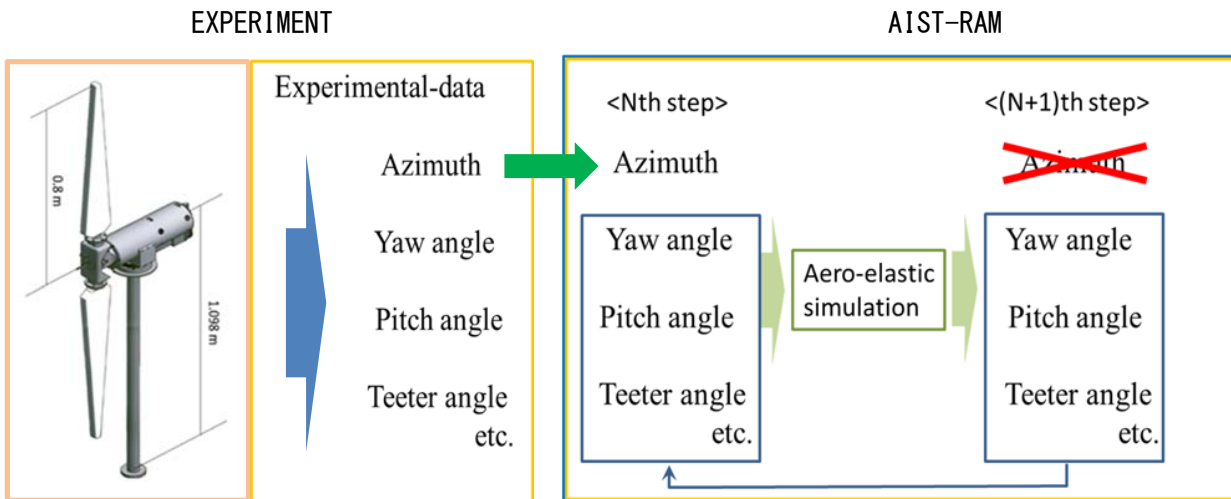
Figure 5 : Main facility of HILS system

   As is shown in Figure 5, between the models running parallel, at some step, for example the azimuth datum is exchanged and becomes common in order to make precise and quick comparison between another data.

   Through these process, as to the experiment, the preciseness or credibility of the data produced by the sensor and the data-processing can be seen, and for the simulation model very precise identification as well as tuning could be established.

6. Dynamic analyses of the two-bladed teetered rotor

6.1 Teetered-rotor

   Teetered-rotor is a kind of technology to support the tail-rotor of the helicopter in order to obtain a dynamic stability.

   In 1980th this kind of concept was applied to design prototypes of Megawatt-scale horizontal axis wind turbine, and accordingly, several studies had been conducted.

   In this study, referring to the basic equations from (16) to (19), basic characteristics of the motion was investigated.

6.2 Effect of the gravitational acceleration

   Figure 6 shows the comparison as to teeter motion between the measurement and simulation result according to the azimuth angle.
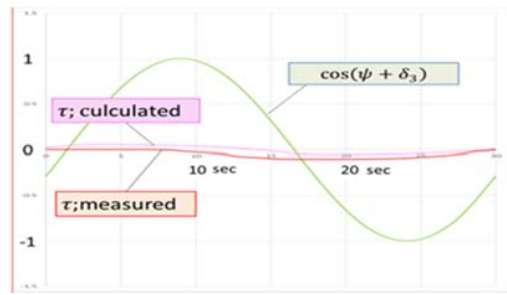
Figure 6 Teeter motion in the case of low-speed by motoring

In this case the rotor is driven by the motor in very low speed of 2 rpm.

According to fifth term of equation (19), effect of the gravity-acceleration is noticeable with a pre-session due to the existence of m_2 and c rerated to the fifth term of equation (16) and the seventh term of equation (17).

Figure 7 shows the result of wind tunnel test under the condition of wind-speed 5 m/s and rotational speed around 100 rpm.
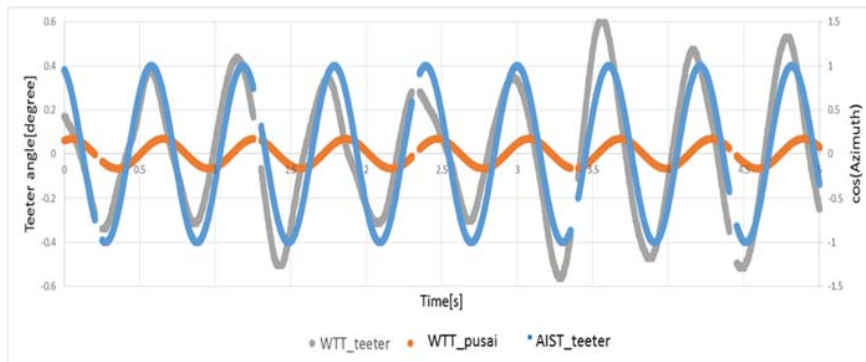
Figure 7 : Comparison between the measurement and simulation as to the teetering motion at wind tunnel test

The result seems identical with the tendency recognized in Figure 6 besides far reduced amplitude of teeter angle due to the effect of centrifugal force by the third term of equation (19).

6.3 Effect of the centrifugal force

Figure 8 shows the comparison as to the amplitude of teetering motion according to the rotational speed of the rotor between the result of simulation and the wind tunnel test.
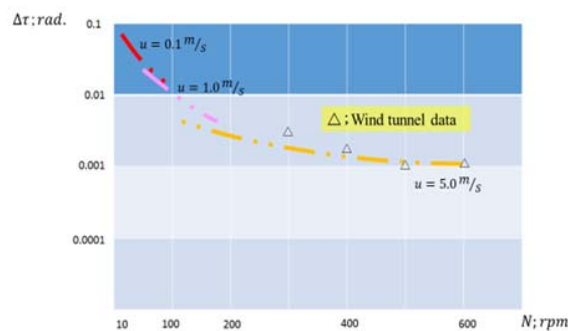
Figure 8 : Comparison of the amplitude of teetered angle according to the rotational speed

6.4 Effect of the wind profile

In order to make a research as to the effect of wind profile, out-door HILS-testing under the natural wind was conducted.

Circumstance of the test was constructed with the measurement of wind-speed not only at hub height but also at the top and foot of the rotor which was implemented to the HILS system.

Figure 9 shows the result.
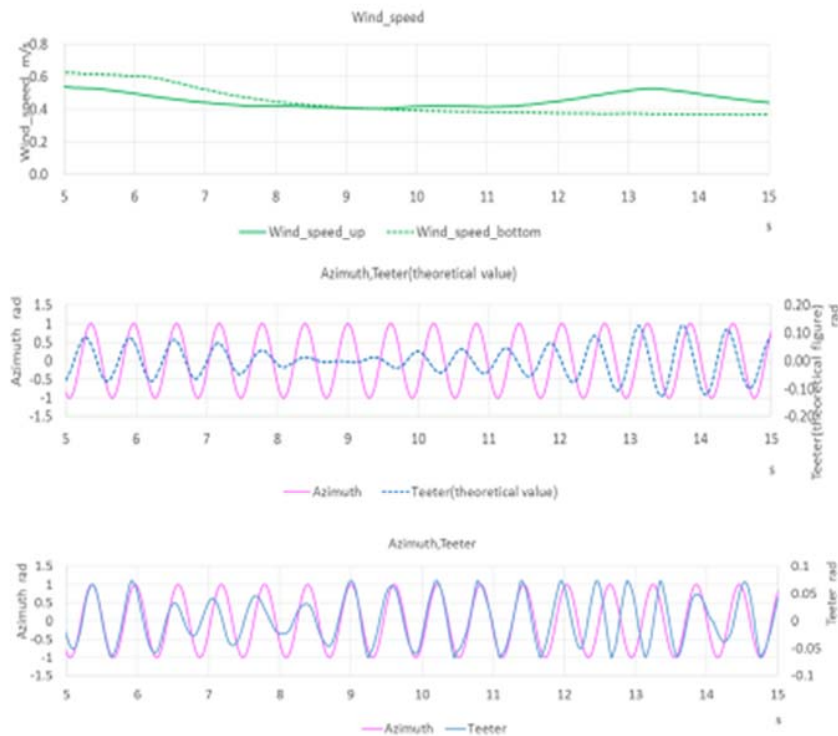
Figure 9 Teetering motion under various wind profile

In this case, at the beginning, wind profile is reverse, namely wind speed at upper area is more week than that of lower area until 8 second, where the profile begin to change to more normal condition.

Under the normal wind profile condition, the effect of wind speed distribution is similar to the effect of gravitational acceleration by which the peak of teeter motion leads the peak of azimuth as is seen at whole of Figure 7 and at Figure 8 from 8 second to 14 second.

While under the reverse wind profile condition as is seen from 5 second to 8 second in Figure 8, the effect of wind profile weaken the effect of the gravitational acceleration that reduce the lead of teeter-peak to the azimuth-peek.

And when the wind profile is neutral at 9 second, the amplitude of teeter motion becomes minimum, because the effect of centrifugal force becomes dominant in these condition.

There are several point where the result of measurement as to teeter angle has some discrepancy to the result of simulation.

Considering these result, modelling of the wind condition around the rotor seems to be most important to establish the precise and credible simulation.

7. Summary

In order to make an approach according to the dynamic characteristics of the two-bladed Horizontal axis wind turbine, that is substantially unstable and non-linear motion, the basic equations were derived by Lagrange's method on Eulerian coordinate system.

An aero-elastic simulation model named AIST-RAM (AIST Real-Time Model), that represents characteristics of the motion was developed referring to the basic equations and another factors such as an aerodynamic force acting on the blades that is strongly affected by the motion and elasticity of the blades itself.

Also, scale model of the multi-megawatt horizontal-axis wind turbine was constructed as well as the specified management system called Hard-wear in the Loop (HIL).

Through the successive evaluation by wind-tunnel testing and field testing accompanied with real-time simulation arranged by the Hard-wear in the Loop System, the simulation model shows significant credibility and preciseness particularly for the inertial property, while as to the effect of the aerodynamic forces, namely to construct the time-domain detailed characteristics of the wind, there remains a problem with significant difficulty to make and implement it to the real-time simulation model.

8. Acknowledgement

This study was supported by Japanese national project that made a study and research work according to the Multi-Megawatt Large scale Horizontal axis Wind turbine.

I would like to appreciate people who involved to the project on behalf of METI, NEDO, AIST and several Academies and Industries.

REFERENCES

1）B.Luhmann, P.W.Cheng

Relevance of aerodynamic modelling for load reduction control strategies of Two-bladed wind turbines

The Science of Making Torque from Wind 2014

2) V Schorbach, P Dalhoff, P Gust

Taming the inevitable : significant parameters of teeter end impacts

The Science of Making Torque from Wind 20

3)John C. Slater, Nathanael H. Frank

Mechanics

McGraw-Hill Book Company 1947

4) J.M.Jonkman and M.L.Buhl, Jr．:

New Development for the NWTC's FAST Aero-elastic HAWT Simulator.

42nd Aerospace Sciences Meeting and Exhibit Conference, NREL/CP-500-35077,2003.